4th International Conference on Science, Technology and Management
India International Centre, New Delhi (ICSTM-16)
15th May 2016, www.conferenceworld.in ISBN: 978-81-932074-8-2

AN ACTIVE POWER FILTER PERFORMANCE IMPROVED BY USING PREDICTIVE CONTROL SCHEME FOR RENEWABLE POWER GENERATION SYSTEMS

Priyanka Baban Bhoyar[1], K. Bahadure[2]

ABSTRACT

An active power filter enforced with a four-leg voltage-source inverter employing a predictive control scheme is presented. The use of a four-leg voltage-source inverter permits the compensation of current harmonic elements, as well as unbalanced current generated by single-phase nonlinear loads. A detailed yet easy mathematical model of the active power filter, together with the result of the equivalent grid impedance, is derived and used to design the predictive control algorithm. The compensation performance of the proposed active power filter and therefore the associated control scheme below steady state and transient operating conditions is demonstrated through simulations and simulation results.

Keywords: Active Power Filter, Current Control, Four-Leg Converters, Predictive Control, Enhanced Phased Locked Loop (EPLL).

I. INTRODUCTION

Renewable generation affects power quality as a result of its nonlinearity, since solar generation plants and wind power generators should be connected to the grid through high-power static PWM converters [1]. The non uniform nature of power generation directly affects voltage regulation and creates voltage distortion in power systems. This new scenario in power distribution systems would require additional sophisticated compensation techniques.

Although active power filters enforced with three-phase four-leg voltage-source inverters (4L-VSI) have already been presented within the technical literature [2]–[6], the first contribution of this paper is also a predictive control algorithm designed and enforced specifically for this application. Historically, active power filters are controlled using pre tuned controllers, like PI-type or adaptative, for the present as well as for the dc-voltage loops [7], [8]. PI controllers should be designed based on the equivalent linear model, whereas predictive controllers use the nonlinear model, which is closer to real operating conditions. an accurate model obtained using predictive controllers improves the performance of the active power filter, particularly throughout transient operating conditions, as a results of it'll quickly follow the current-reference signal whereas maintaining a constant dc-voltage.

This paper presents the mathematical model of the 4L-VSI and also the principles of operation of the proposed predictive control scheme, together with the design procedure. The complete description of the selected current reference generator enforced within the active power filter is also presented. Finally, the proposed active power

filter and also the effectiveness of the associated control theme compensation are demonstrated through simulation and valid with simulation results obtained throughout a 2 kVA laboratory image.

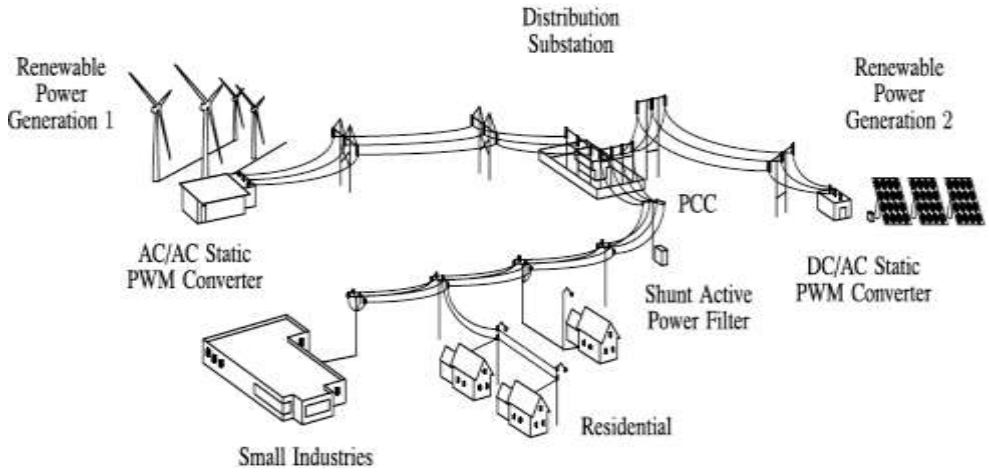

Fig. 1. Stand-alone hybrid power generation system with a shunt active power filter.

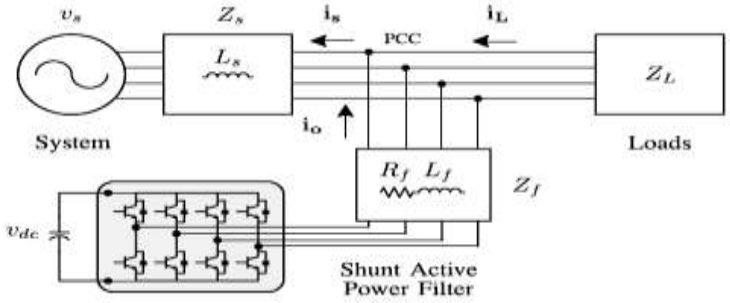

Fig. 2. Three-phase equivalent circuit of the proposed shunt active power filter.

II. FOUR-LEG CONVERTER MODEL

Fig. 1 shows the configuration of a typical power distribution system with renewable power generation. It consists different kinds of power generation units and different kinds of loads. Renewable sources, like wind and sunlight, are generally used to generate electricity for residential users and small industries. Both kinds of power generation use ac/ac and dc/ac static PWM converters for voltage conversion and battery banks for long term energy storage. These converters perform maximum power point tracking to extract the maximum energy attainable from wind and sun. The power consumption behavior is random and unpredictable, and also, it should be single- or three-phase, balanced or unbalanced, and linear or nonlinear. An active power filter is connected in parallel at the point of common coupling to compensate current harmonics, current unbalance, and reactive power. It's composed by an capacitor, a four-leg PWM converter, and a first-order output ripple filter, as shown in Fig. 2. This circuit considers the power system equivalent impedance Zs, the converter output ripple filter impedance Z_f, and also the load impedance Z_L.

The four-leg PWM converter topology is shown in Fig. 3. This converter topology is similar to the conventional three-phase converter with the fourth leg connected to the neutral bus of the system. The fourth leg will increase

switching states from 8 to 16, rising control flexibility and output voltage quality, and is suitable for current unbalanced compensation.

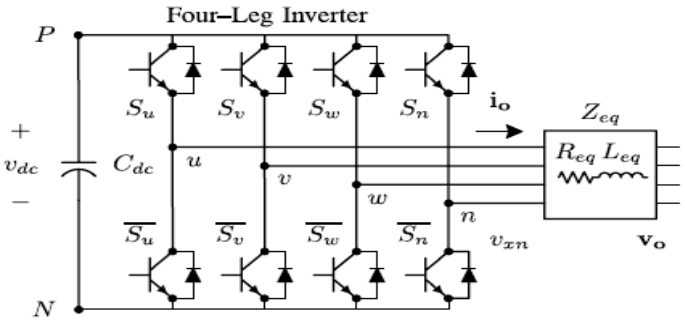

Fig. 3. Two-level four-leg PWM-VSI topology.

The voltage in any leg x of the converter, measured from the neutral point (n), can be expressed in terms of switching states, as follows:

$$V_{xn} = S_x - S_n, \quad x=u, v, w,n. \qquad (1)$$

The mathematical model of the filter derived from the equivalent circuit shown in Fig. 2 is

$$V_o = v_{xn} - R_{eq}\, i_o - L_{eq}\frac{di_o}{dt} \qquad (2)$$

Where R_{eq} and L_{eq} are the 4L-VSI output parameters expressed as Thevenin impedances at the converter output terminals Z_{eq}. Therefore, the Thevenin equivalent impedance is determined by a series connection of the ripple filter impedance Z_f and a parallel arrangement between the system equivalent impedance Z_s and the load impedance Z_L

$$Z_{eq} = \frac{Z_s Z_L}{Z_s + Z_L} + Z_f \approx Z_s + Z_f. \qquad (3)$$

For this model, it is assumed that Z_L »Z_s, that the resistive part of the system's equivalent impedance is neglected, and that the series reactance is in the range of 3–7% p.u., which is an acceptable approximation of the real system. Finally, in (2) $R_{eq} = R_f$ and $L_{eq} = L_s + L_f$.

III. DIGITAL PREDICTIVE CURRENT CONTROL

The diagram of the proposed digital predictive current control scheme is shown in Fig. 4. This control scheme is essentially an optimization algorithm and, therefore, it's to be enforced during a microprocessor. Consequently, the analysis should be developed using discrete mathematics in order to consider about additional restrictions like time delays and approximations.

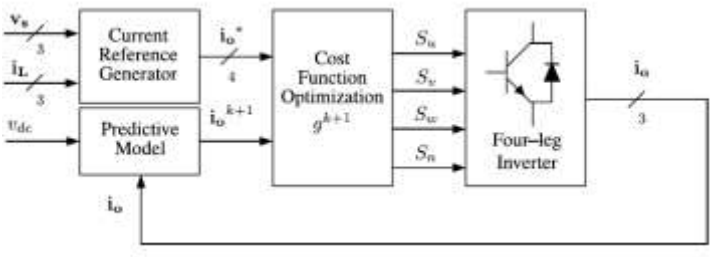

Fig. 4. Proposed predictive digital current control block diagram.

The main characteristic of predictive control is the use of the system model to predict the longer term behavior of the variables to be controlled. The controller uses this information to select the optimum switching state that may be applied to the power converter, according to predefined improvement criteria. The predictive control algorithm is simple to implement and to know, and it may be enforced with 3 main blocks, as shown in Fig. 4.

1) Current Reference Generator: This unit is designed to generate the desired current reference that's used to compensate the undesirable load current elements. During this case, the system voltages, the load currents, and also the dc-voltage converter are measured, whereas the neutral output current and neutral load current are generated directly from these signals (IV).

2) Prediction Model: The converter model is employed to predict the output converter current. Since the controller operates in discrete time, both the controller and also the system model should be represented during a discrete time domain. The discrete time model consists of a recursive matrix equation that represents this prediction system. this implies that for a given sampling time Ts, knowing the converter switching states and control variables at instant kTs, it's attainable to predict the next states at any instant [k + 1]Ts .Due to the first-order nature of the state equations that describe the model in (1)–(2), a sufficiently accurate first-order approximation of the derivative is considered during this paper

$$\frac{dx}{dt} \approx \frac{x[k+1] - x[k]}{T_s}. \qquad (4)$$

The 16 possible output current predicted values can be obtained from (2) and (4) as

$$\mathbf{i_o}[k+1] = \frac{T_s}{L_{eq}}(v_{xn}[k] - \mathbf{v_o}[k]) + \left(1 - \frac{R_{eq}T_s}{L_{eq}}\right)\mathbf{i_o}[k]. \qquad (5)$$

As shown in (5), in order to predict the output current $\mathbf{i_o}$ at the instant (k + 1), the input voltage value $\mathbf{v_o}$ and the converter output voltage v_{xN}, are required. The algorithm calculates all 16 values associated with the possible combinations that the state variables can achieve.

3) Cost Function Optimization: In order to select the optimal switching state that must be applied to the power converter, the 16 predicted values obtained for $\mathbf{i_o}$[k + 1] are compared with the reference using a cost function g, as follows:

$$\begin{aligned} g[k+1] = {} & (i^*_{ou}[k+1] - i_{ou}[k+1])^2 \\ & + (i^*_{ov}[k+1] - i_{ov}[k+1])^2 \\ & + (i^*_{ow}[k+1] - i_{ow}[k+1])^2 \\ & + (i^*_{on}[k+1] - i_{on}[k+1])^2 . \end{aligned} \qquad (6)$$

The output current (io) is equal to the reference (i*o) when g = 0. Therefore, the improvement goal of the value / the price function is to attain a g value near to zero. The voltage vector v_X that minimizes the cost function is chosen and applied at ensuing sampling state. Throughout every sampling state, the switching state that generates the minimum price of g is chosen from the 16 possible function values. The algorithm selects the switching state that produces this lowest value and applies it to the converter throughout the k + 1 state.

International Journal of Advance Research in Science and Engineering
Vol. No.5, Issue No. 05 , May 2016
www.ijarse.com
IJARSE
ISSN 2319 - 8354

IV. CURRENT REFERENCE GENERATION

A dq-based current reference generator scheme is employed to get the active power filter current reference signals. This scheme presents a quick and accurate signal tracking capability. This characteristic avoids voltage fluctuations that deteriorate the current reference signal affecting compensation performance. The current reference signals are obtained from the corresponding load currents as shown in Fig. 5. This module calculates the reference signal currents needed by the converter to compensate reactive power, current harmonic and current imbalance. The displacement power factor (sinφ(L)) and also the maximum total harmonic distortion of the load (THD(L)) defines the relationships between the apparent power needed by the active power filter, with respect to the load, as shown

$$\frac{S_{APF}}{S_L} = \frac{\sqrt{\sin\phi_{(L)} + \mathrm{THD}_{(L)}{}^2}}{\sqrt{1 + \mathrm{THD}_{(L)}{}^2}} \qquad (7)$$

Where the value of THD(L) includes the maximum compensable harmonic current, defined as double the sampling frequency fs. The frequency of the maximum current harmonic element which will be compensated is equal to one 1/2 the converter switching frequency.

The dq-based scheme operates during a rotating reference frame; thus, the measured currents should be increased by the sin(wt) and cos(wt) signals. By using dq-transformation, the d current element is synchronized with the corresponding phase-to-neutral system voltage, and also the letter of the alphabet current element is phase-shifted by 90◦. The sin(wt) and cos(wt) synchronized reference signals are obtained from a EPLL. The EPLL generates a pure sinusoidal waveform even when the system voltage is severely distorted.

V. ENHANCED PHASED LOCKED LOOP (EPLL)

Enhanced phase-locked loop (EPLL) may be a frequency-adaptive nonlinear synchronization approach. The diagram of EPLL is shown in Fig.5. Its major improvement over the conventional PLL lies in the pd mechanism that permits more flexibility and provides additional information like amplitude and phase angle. There are 3 independent internal parameters K, K_p K_v and K_i K_v. Parameter K dominantly controls the speed of the amplitude convergence. K_p K_v and K_i K_v control the rates of phase and frequency convergence.

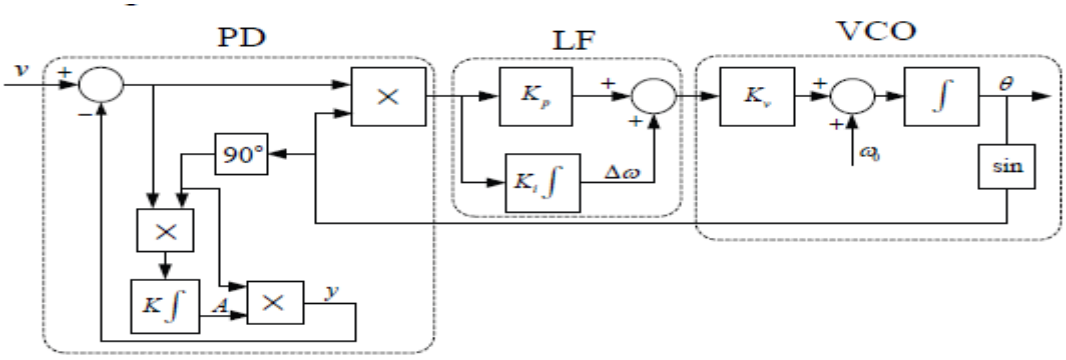

Fig.5 Block diagram of single-phase EPLL

EPLL will give higher degree of immunity and insensitivity to noise, harmonics and unbalance of the signal. It's an efficient method for synchronization of the grid-interfaced converters in impure and variable frequency

environments. Additionally, EPLL will provide the 90 degrees shift of the input signal. Therefore, it's an attractive solution in some single phase system applications.

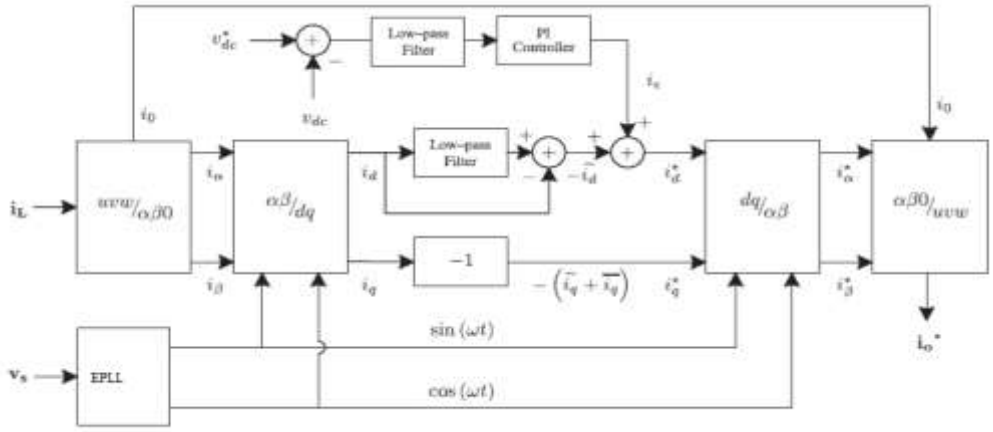

Fig. 6. *dq*-based current reference generator block diagram.

Tracking errors are eliminated, since EPLLs are designed to avoid phase voltage unbalancing, harmonics (i.e., less than 5% and 3% in fifth and seventh, respectively), and offset caused by the nonlinear load conditions and measurement errors Equation (8) shows the relationship between the real currents $i_{Lx}(t)$ (x = u, v,w) and the associated dq components (i_d and i_q)

$$\begin{bmatrix} i_d \\ i_q \end{bmatrix} = \sqrt{\frac{2}{3}} \begin{bmatrix} \sin\omega t & \cos\omega t \\ -\cos\omega t & \sin\omega t \end{bmatrix} \begin{bmatrix} 1 & -\frac{1}{2} & -\frac{1}{2} \\ 0 & \frac{\sqrt{3}}{2} & -\frac{\sqrt{3}}{2} \end{bmatrix} \begin{bmatrix} i_{Lu} \\ i_{Lv} \\ i_{Lw} \end{bmatrix}. \tag{8}$$

A low-pass filter (LFP) extracts the dc element of the phase currents id to get the harmonic reference elements −∼id. The reactive reference elements of the phase-currents are obtained by phase-shifting the corresponding ac and dc components of iq by 180◦. in order to keep the dc-voltage constant, the amplitude of the converter reference current should be changed by adding an active power reference signal ie with the d-component, as will be explained in Section IV-A. The ensuing signals i*d and i*q are transformed back to a three-phase system by applying the inverse Park and Clark transformation, as shown in (9). The cutoff frequency of the LPF used in this paper is 20 Hz.

$$\begin{bmatrix} i^*_{ou} \\ i^*_{ov} \\ i^*_{ow} \end{bmatrix} = \sqrt{\frac{2}{3}} \begin{bmatrix} \frac{1}{\sqrt{2}} & 1 & 0 \\ \frac{1}{\sqrt{2}} & -\frac{1}{2} & \frac{\sqrt{3}}{2} \\ \frac{1}{\sqrt{2}} & -\frac{1}{2} & -\frac{\sqrt{3}}{2} \end{bmatrix} \times \begin{bmatrix} 1 & 0 & 0 \\ 0 & \sin\omega t & -\cos\omega t \\ 0 & \cos\omega t & \sin\omega t \end{bmatrix} \begin{bmatrix} i_0 \\ i^*_d \\ i^*_q \end{bmatrix}. \tag{9}$$

The current that flows through the neutral of the load is compensated by injecting the same instantaneous value obtained from the phase-currents, phase-shifted by 180 ◦, as shown next

$$i_{on}^{*} = -\left(i_{Lu} + i_{Lv} + i_{Lw}\right). \qquad (10)$$

One of the major advantages of the dq-based current reference generator scheme is that it permits the implementation of a linear controller within the dc-voltage control loop. However, one necessary disadvantage of the dq-based current reference frame algorithm used to generate the current reference is that a second order harmonic element is generated in id and iq below unbalanced operating conditions. The amplitude of this harmonic depends on the percent of unbalanced load current (expressed as the relationship between the negative sequence current iL,2 and also the positive sequence current iL,1). The second-order harmonic cannot be removed from id and iq , and therefore generates a 3rd harmonic within the reference current when it's converted back to abc frame Fig.7 shows the percent of system current imbalance and therefore the percent of third harmonic system current, in operate of the percent of load current imbalance. Since the load current doesn't have a 3rd harmonic, the one generated by the active power filter flows to the facility system

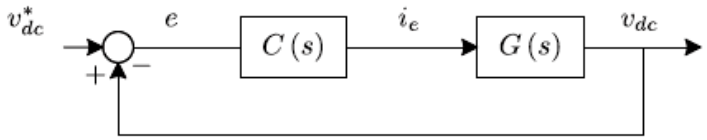

Fig. 7. DC-voltage control block diagram.

5.1 DC-Voltage Control

The dc-voltage converter is controlled with a conventional PI controller. This can be a very important issue within the analysis, since the value function (6) is designed using only current references, in order to avoid the use of weighting factors. Generally, these weighting factors are obtained, and they are not well defined when different operating conditions are needed. In addition, the slow dynamic response of the voltage across the electrolytic capacitor doesn't have an effect on the current transient response. For this reason, the PI controller represents an easy and effective alternative for the dc-voltage control.

The dc-voltage remains constant (with a minimum value of √6vs (rms)) till the active power absorbed by the converter decreases to A level wherever it's unable to compensate for its losses. The active power absorbed by the converter is controlled by adjusting the amplitude of the active power reference signal ie, that is in phase with each phase voltage. In the diagram shown in Fig. 5, the dc-voltage vdc is measured then compared with a constant reference value v*dc. The error (e) is processed by a PI controller, with 2 gains, Kp and Ti .Both gains are calculated consistent with the dynamic response requirement. Fig. 7 shows that the output of the PI controller is fed to the dc voltage transfer function Gs, that is represented by a first-order system (11)

$$G(s) = \frac{v_{\mathrm{dc}}}{i_e} = \frac{3}{2}\frac{K_p v_s \sqrt{2}}{C_{\mathrm{dc}} v_{\mathrm{dc}}^{*}}. \qquad (11)$$

The equivalent closed-loop transfer function of the given system with a PI controller (12) is shown in (13)

$$C(s) = K_p\left(1 + \frac{1}{T_i \cdot s}\right) \qquad (12)$$

$$\frac{v_{\mathrm{dc}}}{i_e} = \frac{\frac{\omega_n^2}{a} \cdot (s+a)}{s^2 + 2\zeta\omega_n \cdot s + \omega_n^2}. \qquad (13)$$

Since the time response of the dc-voltage control loop does not need to be fast, a damping factor ζ = 1and a natural angular speed $\omega_n = 2\pi \cdot 100$ rad/s are used to obtain a critically damped response with minimal voltage oscillation. The corresponding integral time $T_i = 1/a$ (13) and proportional gain K_p can be calculated as

$$\zeta = \sqrt{\frac{3}{8}\frac{K_p v_s \sqrt{2} T_i}{C_{dc} v_{dc}^*}} \qquad (14)$$

$$\omega_n = \sqrt{\frac{3}{2}\frac{K_p v_s \sqrt{2}}{C_{dc} v_{dc}^* T_i}}, \qquad (15)$$

TABLE I
SPECIFICATION PARAMETERS

Variable	Description	Value [a]
$\mathbf{v_s}$	Source voltage	55 $[V]$
f	System frequency	50 $[Hz]$
v_{dc}	dc-voltage	162 $[V]$
C_{dc}	dc capacitor	2200 $[\mu F]$ (2.0 pu)
L_f	Filter inductor	5.0 $[mH]$ (0.5 pu)
R_f	Internal resistance within L_f	0.6 $[\Omega]$
T_s	Sampling time	20 $[\mu s]$
T_e	Execution time	16 $[\mu s]$

[a]Note: V_{base} = 55 V and S_{base} = 1 kVA.

VI. SIMULATION RESULTS

A simulation model for the three-phase four-leg PWM converter with the parameters shown in Table I has been developed using MATLAB-Simulink. The objective is to verify the current harmonic compensation effectiveness of the proposed control scheme under different operating conditions. A six-pulse rectifier was used as a nonlinear load.

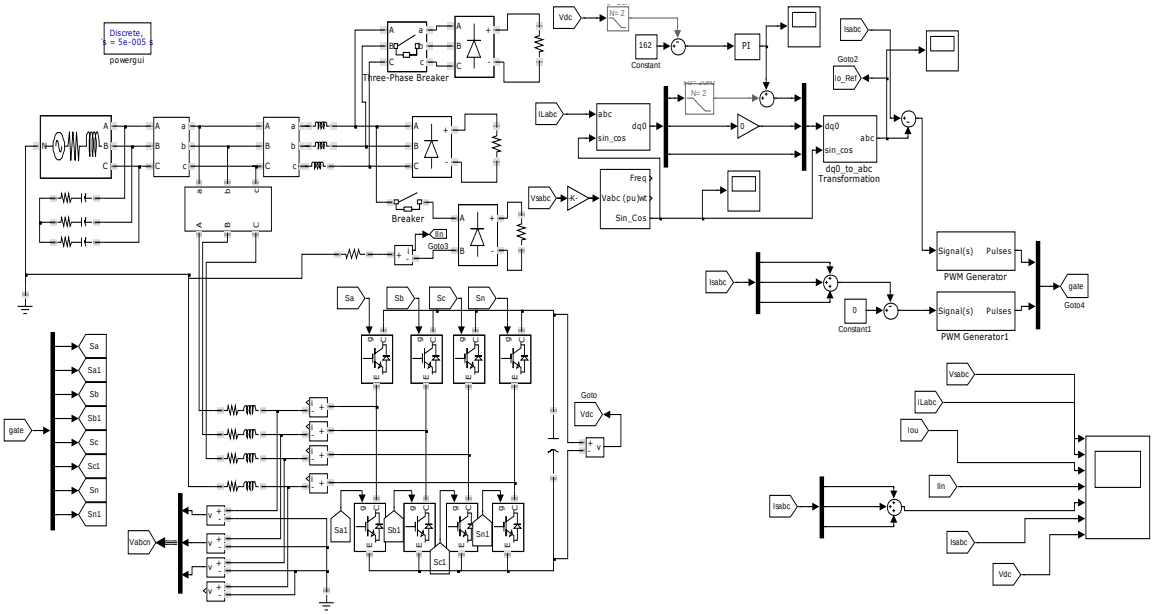

Fig.7 Simulation model for the proposed circuit

International Journal of Advance Research in Science and Engineering
Vol. No.5, Issue No. 05 , May 2016
www.ijarse.com
IJARSE
ISSN 2319 - 8354

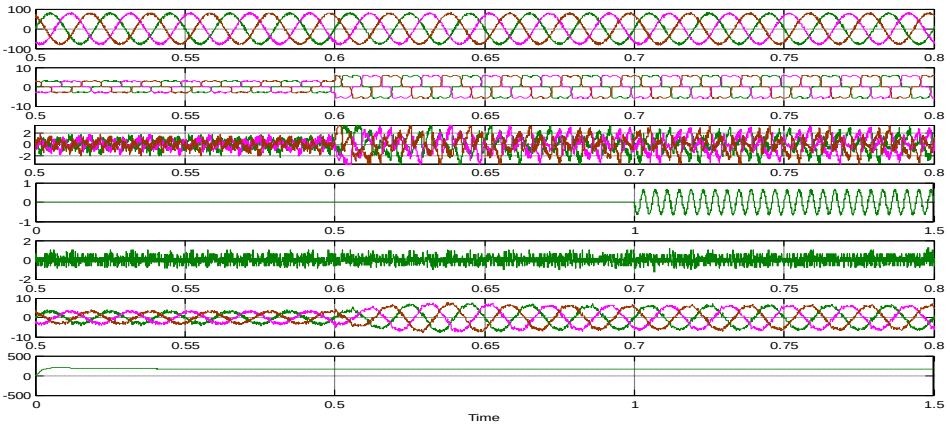

Fig.8. Source voltage (V_{sabc}), Load current (I_{Labc}), Filter output currents (I_{cabc}), load neutral current (ILn), system neutral current (Isn), system currents (Isabc), dclink voltage (Vdc)

In the simulated results shown in Fig.7, the active filter starts to compensate at t = t_1. At this time, the active power filter injects an output current i_{ou} to compensate current harmonic components, current unbalanced, and neutral current simultaneously.

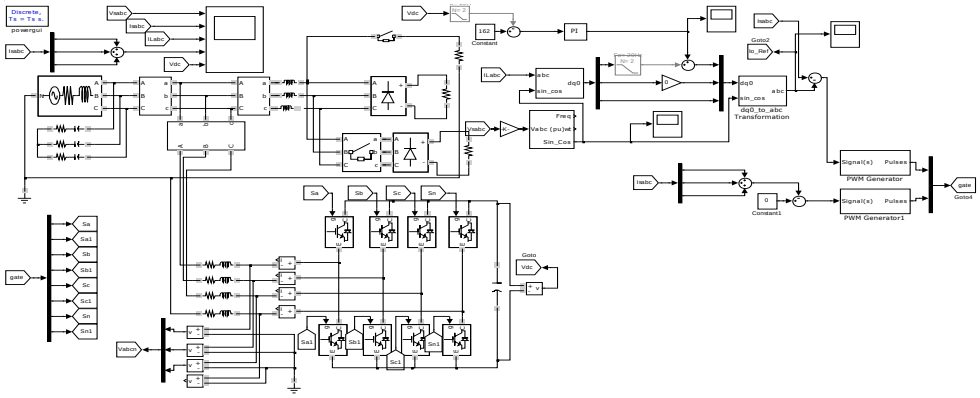

Fig . 9. Simulation model of proposed system

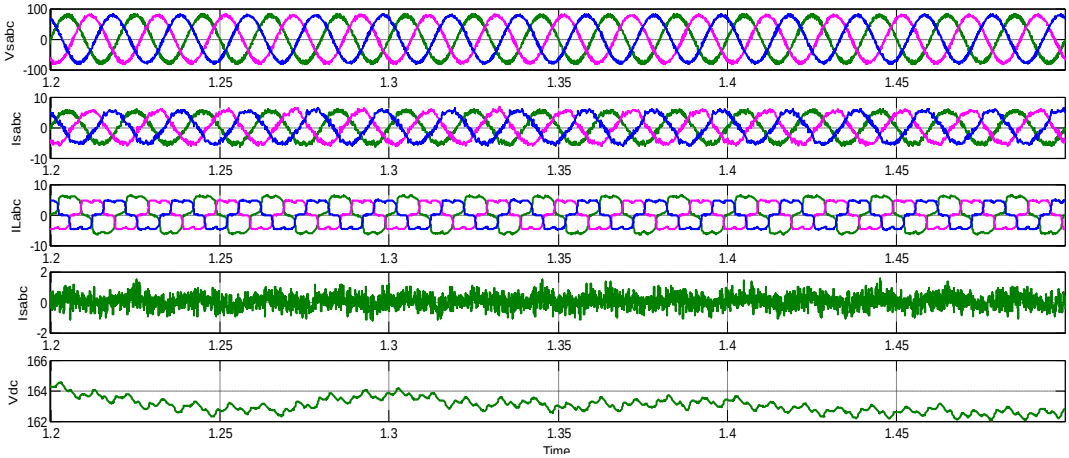

Fig .10 Source voltage, Load current, Filter output currents, load neutral current, system neutral current, system currents, dc link voltage

VII. CONCLUSION

Improved dynamic current harmonics and a reactive power compensation scheme for power distribution systems with generation from renewable sources has been proposed to improve the current quality of the distribution system. Advantages of the proposed scheme are associated with its simplicity, modeling, and implementation. The use of a predictive control algorithm for the converter current loop proved to be an efficient solution for active power filter applications, improving current tracking capability, and transient response. Simulation results have proved that the proposed predictive control algorithm may be a good various to classical linear control methods. The predictive current control algorithm may be a stable and robust solution. Simulation results have shown the compensation effectiveness of the proposed active power filter.

REFERENCES

[1] J. Rocabert, A. Luna, F. Blaabjerg, and P. Rodriguez, "Control of power converters in AC microgrids," IEEE Trans. Power Electron., vol. 27, no. 11, pp. 4734–4749, Nov. 2012.

[2] M. Aredes, J. Hafner, and K. Heumann, "Three-phase four-wire shunt active filter control strategies," IEEE Trans. Power Electron., vol. 12, no. 2, pp. 311–318, Mar. 1997.

[3] S. Naidu and D. Fernandes, "Dynamic voltage restorer based on a fourleg voltage source converter," Gener. Transm. Distrib., IET, vol. 3, no. 5, pp. 437–447, May 2009.

[4] N. Prabhakar and M. Mishra, "Dynamic hysteresis current control to minimize switching for three-phase four-leg VSI topology to compensate nonlinear load," IEEE Trans. Power Electron., vol. 25, no. 8, pp. 1935– 1942, Aug. 2010.

[5] V. Khadkikar, A. Chandra, and B. Singh, "Digital signal processor implementation and performance evaluation of split capacitor, four-leg and three h-bridge-based three-phase four-wire shunt active filters," Power Electron., IET, vol. 4, no. 4, pp. 463–470, Apr. 2011.

[6] F. Wang, J. Duarte, and M. Hendrix, "Grid-interfacing converter systems with enhanced voltage quality for microgrid application; concept and implementation," IEEE Trans. Power Electron., vol. 26, no. 12, pp. 3501– 3513, Dec. 2011.

[7] X.Wei, "Study on digital pi control of current loop in active power filter," in Proc. 2010 Int. Conf. Electr. Control Eng., Jun. 2010, pp. 4287–4290.

[8] R. de Araujo Ribeiro, C. de Azevedo, and R. de Sousa, "A robust adaptive control strategy of active power filters for power-factor correction, harmonic compensation, and balancing of nonlinear loads," IEEE Trans. Power Electron., vol. 27, no. 2, pp. 718–730, Feb. 2012.